RESEARCH ARTICLE

Editorial Process: Submission:05/23/2025 Acceptance:02/17/2026 Published:03/05/2026

Cytotoxic and Apoptotic Effects of Compounds Isolated from *Atalantia monophylla* Peels on Human Cancer Cell Lines

Pichit Sudta[1]*, Jantana Yahuafai[2], Vatcharaporn Prapasanobol[1], Phurpa Wangchuk[3]

Abstract

Objective: This study aimed to extract and purify compounds from traditional Thai medicine, *A. monophylla* peels, and evaluate their antiproliferative and mechanistic effects. **Methods:** Peels of *A. monophylla* were extracted using various solvents. Compounds were isolated using column chromatography and preparative thin-layer chromatography. Structural elucidation was performed using spectroscopic techniques and by comparison with literature data. Antiproliferative activity was assessed using the MTT assay against several human cancer cell lines (MCF-7, HeLa S3, HepG2,HCT116) and normal Vero cells. Apoptosis and cell cycle arrest were evaluated using Hoechst 33342 staining and flow cytometry with annexin V/PI staining. **Result:** The acetone extract and its sub-fractions showed potent antiproliferative effects, particularly against MCF-7 breast cancer cells. In contrast, n-hexane and methanol extracts were less active. Bioactivity-guided fractionation yielded two benzoyl tyramine alkaloids: servarine palmitate (1) and acidissiminol epoxide (2), with the latter displaying the highest cytotoxicity. Mechanistic studies revealed hallmark apoptotic features, including membrane blebbing, chromatin condensation, nuclear fragmentation, apoptotic body formation, and loss of adhesion. Additionally, acidissiminol epoxide (2) induced G0/G1 cell cycle arrest, suggesting disruption of DNA synthesis and activation of apoptotic pathways. **Conclusion:** This study reports, for the first time, the isolation of tyramine alkaloid 2 from *A. monophylla* and its potent anticancer activity against breast cancer cells. These findings highlight its potential as a lead compound for the development of novel epoxide-containing anticancer agents.

Keywords: *Atalantia monophylla*- acetone extract- acidissiminol epoxide- anticancer activity- apoptosis induction

Asian Pac J Cancer Prev, **27 (3)**, 867-875

Introduction

Cancer is a chronic disease and continues to be one of the leading causes of death worldwide [1]. Despite novel developments in cancer therapy, advancements in medication, and revolutionary progress in genomics and molecular biology, multidrug resistance remains a significant challenge, as well as serious side effects of drugs are still important causes of the failure of cancer treatment [2]. Plants have been used for a long time in cancer treatment and serve as rich sources of natural compounds, many of which have led to the development of effective anticancer agents that are currently used [3]. However, the search for new compounds that more specifically target cancer cells without side effects from medicinal plants remains a challenging strategy for new anticancer drug discovery [4].

Atalantia monophylla (family Rutaceae) is a tropical medicinal shrub that widely grows in the mountainous regions of some countries, including South India, Sri Lanka, Southeast Asia, and Thailand [5-7]. This plant has been used in folk medicine for several purposes, especially in Thai herbal medicine, and the leaves of this plant have a scent similar to that of kaffir lime or lemon leaves. They are used to treat respiratory diseases, relieve colic, alleviate diarrhea, and address skin conditions. The fruit is not edible but is also utilized for respiratory ailments, while oil extracted from the peel is applied externally to treat rheumatoid arthritis [8]. Previous pharmacological studies of *A. monophylla* extracts have demonstrated a range of biological activities, including antifeedant, repellent, antigenotoxic, antioxidant, immunomodulatory, antifungal, and apoptotic effects [9-12]. Several studies on the chemical constituents of *A. monophylla* revealed that limonoids, acridone alkaloids, furoquinoline alkaloids [12, 13], coumarins, and flavonoids [14] are present in different parts of the plant. The peels of *A. monophylla* seem to be a rich source of benzoyltyramine alkaloids with cytotoxic activity [15, 16]. However, the major chemical constituents with specific anticancer activity

*[1]Division of Chemistry, Faculty of Science and Technology, Phetchaburi Rajabhat University, Phetchaburi, Thailand. [2]Division of Research and Technology Assessment, National Cancer Institute, Bangkok, Thailand. [3]College of Science and Engineering, James Cook University, Cairns campus, Smithfield, QLD, Australia. *For Correspondence: pichit.sud@mail.pbru.ac.th*

against *A. monophylla* peels remain unclear. In this study, we evaluated the antiproliferative effects of three total crude extracts, four acetone-derived subfractions, and two major isolated compounds from *A. monophylla* peels on breast cancer cells. Mechanistic investigations further revealed the ability of the compounds to induce apoptosis, as demonstrated through cell cycle arrest and apoptosis assays.

Materials and Methods

Chemicals

Doxorubicin, an anticancer drug, was obtained from Merck. 3-(4,5-Dimethylthiazol-2-yl)-2,5-dimethyl-tetrazolium bromide (MTT), propidium iodide (PI), ribonuclease A, and dimethylsulfoxide (DMSO) were purchased from Sigma-Aldrich Chemical Co. (St. Louis, MO, USA). Dulbecco's modified Eagle's medium (DMEM), minimum essential medium (MEM), fetal bovine serum (FBS), penicillin and streptomycin, and phosphate-buffered saline (PBS) were obtained from Gibco Life Technologies Inc. (Rockville, MA, USA). The Annexin V/ PI-FITC apoptosis detection kit was from BD Biosciences (San Diego, CA, USA). The Hoechst 33342 staining kit was purchased from Invitrogen (Life Technologies Corp., USA). All other reagents and chemicals used were of the highest purity grade available.

Plant materials

The peels of *A. monophyla* were collected in May 2022 from the Nongkapu Subdistrict, Ban Lat District, Phetchaburi Province, Thailand. The plant was confirmed by comparison with a botanically identified voucher specimen UBUPH01126 at the Faculty of Pharmaceutical Sciences, Ubon Ratchathani University, Ubon Ratchathani Province, and the voucher sample (PBRU-003) was deposited in the collection of the Natural Product Research Unit, Faculty of Science and Technology, Phetchaburi Rajabhat University.

Preparation of crude extracts of A. monophylla

The air-dried powdered peels (3.0 kg) of *A. monophylla* were sequentially extracted by maceration for 5 days at room temperature with hexane (5 x 8 L), acetone (8 x 10 L), and MeOH (5 x 8 L). The macerates were concentrated under reduced pressure to obtain three dry extracts: crude hexane (dark green sticky solid, 235 g), acetone (pale green solid, 326 g), and MeOH (dark green sticky solid, 370 g).

Extraction and isolation

All the extracts were screened for in vitro cytotoxic activity against human breast adenocarcinoma (MCF-7), human cervical carcinoma (HelaS3), human colon carcinoma (HTC116), hepatocarcinoma (HepG2), and Vero cells (normal cells) via the MTT assay. The most active acetone extract was further purified using the column chromatographic method and eluted with a gradient system of hexane, hexane: chloroform, and chloroform: acetone. Based on their TLC characteristics (R_f values and color with the dye), the fractions that contained the same major compounds were combined to yield four fractions, F1-F4. These fractions were subsequently tested for cytotoxicity; fractions F2 and F3 exhibited preferential cytotoxic activity (Table 1), leading to the further isolation of the major constituents. Fraction F2 was purified by silica gel column chromatography and eluted with a gradient system of hexane, hexane: chloroform, and chloroform: acetone to obtain five subfractions, F2.1-F2.5. Subfraction F2.3 was purified by FCC using 5% chloroform: hexane (% v/v) as the eluent to afford two subfractions, F2.3.1 and F2.3.2. Subfraction F2.3.2 was recrystallized in 20% chloroform: hexane (% v/v), affording the known compound, servarine palmitate (1, 128.5 mg, 0.00428%), which has been previously reported from Rutaceae plants, *Severinia buxifolia, Pamburus missionis*, and *A. monophyla* [15, 17]. Fraction F3 was purified by silica gel CC and eluted with a gradient system of hexane, hexane: chloroform, and chloroform: acetone to obtain four subfractions, F3.1-F3.4. Subfraction F3.4 was rechromatographed on FCC by silica gel eluted with 15% chloroform: hexane (v/v) to yield a known alkaloid, acidissiminol epoxide (2, 34.1 mg, 0.00113%), which was previously isolated from *Limonia acidissima* [18]. The purities of compounds 1 and 2 were determined by high-performance liquid chromatography (HPLC) using a Thermo Spectra Series Complete HPLC

Table 1. Cytotoxicity (IC_{50} in mg/mL) and Selectivity Index (SI) of the Extracts, Fractions, and Isolated Compounds from *A. monophylla*

Extracts, Fractions, and compounds	IC_{50} (mg/mL)								
	HelaS3	SI	MCF-7	SI	HepG2	SI	HCT116	SI	Vero
Hexane	306.45 ± 5.85	0.45	318.70 ± 33.84	0.43	525.41 ±7.36	0.26	628.63 ±30.44	0.22	138.05 ±2.35
Acetone	50.18 ±2.05	9.88	46.26 ±1.84	10.71	58.87 ±9.9	8.42	174.98 ±17.58	2.83	495.65 ± 11.68
Methanol	867.40 ±24.04	-	505.18 ±68.14	-	818.07±17.32	-	935.01 ±14.36	-	> 1000
Fraction F1	236.55± 10.06	0.76	132.66± 14.61	1.36	59.80 ±3.58	3.02	129.29 ±5.37	1.4	180.74 ±6.71
Fraction F2	224.94± 16.70	0.17	59.31 ± 11.75	0.66	5.50 ±0.32	7.13	6.75 ±0.32	5.81	39.21 ±6.51
Fraction F3	145.78 ±1.75	0.44	31.67 ±4.58	2.01	4.91 ±0.34	12.93	8.69 ±0.61	7.31	63.51 ±1.29
Fraction F4	106.55 ±6.83	3.69	136.70 ±	2.87	191.33±11.8	2.05	112.94 ±24.87	3.48	392.92 ±33.6
Compound 1	59.59 ±0.95	8.94	57.91 ±1.3	9.2	53.33 ±0.61	9.99	197.23 ±6.79	2.7	532.57 ± 12.61
Compound 2	3.34 ±0.38	11.11	2.52 ±0.42	14.71	5.07 ±0.09	7.31	10.40 ±1.55	3.56	37.07 ±1.62
Doxorubicin	0.065± 0.01	54.15	0.17±0.01	20.7	1.87 ±0.24	1.88	0.35±0.05	10.05	3.52 ± 0.26

The data are expressed as the mean ± SDs of three independent experiments. *SI value > 3 indicates hight selectivity [19]

system (AS3000 autosampler, P4000 pump, UV1000 detector, SN4000 controller; Thermo Fisher Scientific, USA). Chromatographic separation was performed on a BDS Hypersil C18 column (150 mm × 4.6 mm, 5 µm) maintained at 25 °C, with a flow rate of 1.0 mL/min. Detection was carried out at 273 nm. The mobile phase consisted of solvent A (acetonitrile: 0.1% formic acid in water = 80:20, v/v) and solvent B (methanol), and the elution was performed under isocratic conditions at a ratio of 15% A: 85% B for 20 min. The chemical structures of compounds 1 and 2 are presented in Figure 1.

Servarine palmitate (1); White solid (m.p. 112-114 °C (lit; 112-113 °C [17]; R_f 0.3 (30% v/v, acetone:hexane); Purity: 91.29%, t_R 11.64 min; IR ν_{max} (neat); 3345, 2921, 2852, 1731, 1640, 1532, 1236, 1105 cm^{-1}; ^{1}H-NMR (300 MHz, $CDCl_3$) δ: 0.87 (3H, t, *J*= 6.6 Hz, H-16′), 1.21 (3H, s, H-8), 1.22 (3H, s, H-9), 1.28 (24H, m, H-4′-H-15′), 1.61 (2H, brquint, *J*= 6.3 Hz, H-3′), 1.78 (3H, s, H-10), 1.91 (2H, dt, *J*= 1.8, 6.6 Hz, H-5), 2.34 (2H, t, *J*= 6.3 Hz, H-2′), 2.70 (^{1}H, t, *J*= 6.0 Hz, H-6), 2.86 (2H, t, *J*= 7.4 Hz, H-7″), 3.58 (2H, t, *J*= 7.4 Hz, H-8″), 4.62 (2H, d, *J*= 6.0 Hz, H-1), 5.37 (^{1}H, t, *J*= 6.6 Hz, H-4), 5.76 (^{1}H, t, *J*= 6.0 Hz, H-2), 6.87 (2H, d, *J*= 2.8 Hz, H-3″ and H-5″), 7.18 (2H, d, *J*= 2.8 Hz, H-2″ and H-6″), 7.46 (2H, m, H-3‴ and H-5‴), 7.50 (^{1}H, m, H-4‴), 7.84 (2H, dd, *J*= 1.4, 5.0 Hz, H-2‴ and H-6‴); ^{13}C-NMR (75 MHz , $CDCl_3$) δ: 13.1 (C-16′), 14.1 (C-10), 18.8 (C-8), 22.6 (C-15′), 24.6 (C-9), 24.9 (C-3′), 29.1-29.7 (C-4′-C-14′), 32.6 (C-5), 34.5 (C-2′), 34.8 (C-7″), 41.3 (C-8″), 57.8 (C-7), 60.7 (C-6), 64.1 (C-1), 75.4 (C-4), 114.9 (C-2″ and C-6″), 122.8 (C-2), 126.8 (C-2‴ and C-6‴), 128.5 (C-3‴ and C-5‴), 129.7 (C-3″ and C-5″), 131.1 (C-4‴), 131.3 (C-4″), 134.7 (C-1‴), 137.3 (C-3), 157.3 (C-1″), 167.4 (C-9″), 172.8 (C-1′); HRESIMS m/z 670.4452 $[M + Na]^+$ (calcd for $C_{41}H_{61}NNaO_5$, 670.4441).

Acidissiminol epoxide (2); White solid (m.p. 148-149 °C (lit; 146-149 °C [18]; R_f 0.1 (30% v/v, acetone:hexane); Purity: 99.83%, t_R 1.84 min; IR ν_{max} (neat); 3416, 3329, 2987, 2931, 2871, 1637, 1534, 1234, 1009 cm^{-1}; ^{1}H-NMR (300 MHz, $CDCl_3$) δ: 1.28 (3H, s, H-8), 1.31 (3H, s, H-9), 1.75 (3H, s, H-10), 1.90 (2H, dt, *J*= 5.1, 6.6 Hz, H-5), 2.85 (^{1}H, br t, *J*= 6.6 Hz, H-6), 2.86 (2H, d, *J*= 8.5 Hz, H-7′), 3.66 (2H, t, *J*= 6.8 Hz, H-8′), 4.31 (^{1}H, t, *J*= 5.1 Hz, H-4), 4.57 (2H, d, *J*= 6.2 Hz, H-1) 5.80 (^{1}H, brt, *J*= 6.2 Hz, H-2), 6.86 (2H, brd, *J*= 8.5 Hz, H-2′ and H-6′), 7.14 (4H, m, H-3′, H-5′, H-3″and H-5″), 7.48 (^{1}H, m, H-4″), 7.68 (2H, dd, *J*= 1.4, 6.9 Hz, H-2″and H-6″); ^{13}C-NMR (75 MHz, $CDCl_3$) δ: 12.4 (C-10), 18.9 (C-9), 24.6 (C-8), 34.1 (C-5), 34.7 (C-7′), 41.3 (C-8′), 58.1 (C-7), 62.2 (C-6), 64.5 (C-1), 75.2 (C-4), 144.9 (C-2′ and C-6′), 121.1 (C-2), 126.8 (C-2″ and C-6″), 129.8 (C-3″ and C-5″), 131.1 (C-4′), 131.4 (C-4″), 134.6 (C-1″), 141.4 (C-3), 157.4 (C-1′), 167.7 (C-9′); HRESIMS m/z 432.2156 $[M + Na]^+$ (calcd for $C_{25}H_{31}NNaO_4$, 432.2145).

Cell lines and culture

The HeLaS3 (human cervical carcinoma), MCF-7 (human breast cancer), HepG2 (hepatocellular carcinoma), HCT116 (human colon cancer), and Vero (African green monkey kidney) cell lines were purchased from the American Type Culture Collection (ATCC, Manassas, VA, USA). HeLaS3 and HCT116 cells were cultured in DMEM, while MCF-7, HepG2, and Vero cells were maintained in MEM. All media were supplemented with 10% fetal bovine serum (FBS), 100 µg/mL penicillin, and 100 µg/mL streptomycin. The cells were incubated in a humidified atmosphere containing 5% CO_2 at 37°C.

Cell proliferation assay

The proliferation of cancer cells and normal cells was determined via the use of three extracts, fractions (F1- F4), and isolated compounds at different concentrations for 72 hours. Briefly, cells were seeded in 96-well plates at a density of a 3×10^3 cells/well and incubated at 37°C for 24 hours. The cells were subsequently treated with three extracts, subfractions (F1- F4), and two pure compounds at concentrations ranging from 0 to 1000 µg/mL for 72 hours. Doxorubicin (0.03-30 µg/mL) and 0.1% DMSO served as positive and negative controls, respectively. After incubation, the culture medium was discarded, MTT was added, and the mixture was incubated for 3 hours at 37°C. Following this incubation period, the medium was removed, and 100 µL of DMSO was added to each well. Cell viability was measured at 550 nm via a microplate reader. Each drug concentration was tested in six wells across three independent experiments. Cell viability was calculated and expressed as the IC_{50} value. The selectivity index (SI) was calculated by dividing the IC_{50} value for normal cells (Vero) by the IC_{50} value for cancerous cells (SI = IC_{50} of the compound on normal cells/IC_{50} of the compound on cancerous cells. The SI value indicates the sample's selectivity for the tested cell lines. Samples with an SI > 3 were considered to have a high selectivity for cancerous cells [19].

Morphological assessment of cells via phase contrast light and fluorescence microscopy

Hoechst 33342 staining was performed to observe

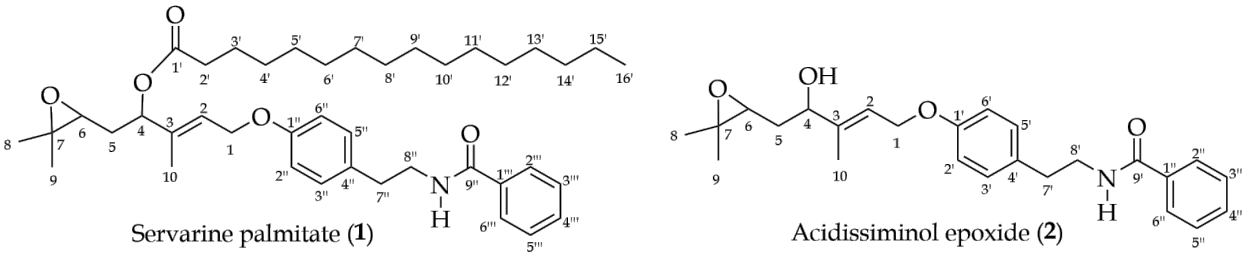

Figure 1. Structures of Known Benzoyl Tyramine Alkaloids 1 and 2

changes in nuclear morphology. Briefly, MCF-7 cells were seeded at a density of 1x105 cells/mL in 6-well plates with cover glasses and incubated for 24 h at 37°C. The cells were subsequently treated with compound 2 at four different concentrations. After a 24-hours of treatment, morphological changes in the MCF-7 cells were observed under an inverted light microscope with phase contrast. Then, the cells were stained with 5 µg/mL Hoechst 33342 for 20 min at room temperature. The slides were washed with PBS, and mounting fluid was applied. A cover slip was placed over the slides, which were then sealed with nail polish. Finally, the cells were imaged under a fluorescence microscope (Nikon, Yokohama, Japan).

Cell cycle analysis by flow cytometry

To analyze the cell cycle distribution in treated cells, MCF-7 cells were treated with 0.1% DMSO or 2 (10, 30, 100, and 300 µg/mL) for 24 h. At the end of the incubation period, both detached and adherent cells were harvested, washed twice with PBS, and fixed overnight in ice-cold 70% ethanol at -20°C. The cell pellets were subsequently washed with PBS, resuspended in ribonuclease A solution, and incubated for 20 minutes at 37°C. Cellular DNA was labeled with propidium iodide (PI) (100 µg/ml) in PBS for at least 30 min in the dark at room temperature and then filtered through a 40 mm nylon filter. The cell cycle distribution was analyzed by flow cytometry using a BD FACSCanto™ II flow cytometer and FACSDiva 6.1.1 software (Becton Dickinson, San Jose, CA, USA).

Apoptosis assay

The number of apoptotic cells was determined via an Annexin V-FITC apoptosis detection kit. Briefly, MCF-7 cells were treated with 2 (10, 30, 100, and 300 µg/mL) for 24 hours. The cells were then collected, washed twice with cold PBS, and resuspended in 500 µL of binding buffer. Subsequently, 5 µL of Annexin V-FITC and 5 µL of PI were added to the cells, followed by incubation in the dark for 10 minutes at 37°C. The stained cells were analyzed using a flow cytometer (BD FACSCanto™ II), and the data were analyzed via FACSDiva 6.1.1 software.

Statistical analysis

The data are expressed as the mean ± standard deviation (S.D.). Differences between groups were evaluated by one-way ANOVA with Dunnett′s multiple comparison test with SPSS statistical software version 23. Differences were considered statistically significant at $p<0.05$.

Results

Structural characterization of the isolated compounds

The chemical structures of the isolated compounds were elucidated based on spectroscopic analyses, including IR, 1D (^{1}H, ^{13}C, DEPT-135), and 2D (COSY, HMQC, HMBC) NMR, and HR-ESI-MS, in comparison with previously.

Compound 1 was obtained as an amorphous white solid with a purity of 91.29%, as determined by HPLC analyses. Its molecular formula, $C_{41}H_{61}NO_5$, was established by HR-ESI-MS (m/z 670.4452 $[M+Na]^+$; calcd. 670.4441). The IR spectrum displayed strong absorption bands corresponding to an ester carbonyl group (1731 cm^{-1}) and an amide carbonyl group (1640 cm^{-1}). The NMR data revealed that 1 consists of two major substructures. The first is the benzoyl tyramine moiety: two doublets at δ7.18 (2H, H-2″ and H-6″) and δ 6.87 (2H, H-3″ and H-5″) indicate a para-substituted character of the benzene ring (C-1″ and C-4″). The HMQC correlations of the methylene protons at δ 2.86 (H-7″) and 3.58 (H-8″) with carbons at δ 34.8 (C-7″) and downfield of the C-N carbon at δ 41.3 (C-8″) confirm the ethylene linkage. In the HMBC spectrum, the correlations of H-7″ and H-8″ with the quaternary aromatic carbon at δ 34.8 (C-4″) demonstrate the attachment of the ethylene moiety to the benzene ring at C-4″, which is consistent with a tyramine unit. The correlation of H-8″ with a benzamide carbonyl (δ 167.4, C-9″) further connects the ethyl group of the tyramine unit to the benzoyl fragment (five aromatic protons at δ 7.84 (H-2‴ and H-6‴), δ7.46 (H-3‴ and H-5‴), and δ 7.50 (H-4‴)). The second substructure involves an O-substituted tyramine unit at C-1″ (δ 157.3). A methylene group at δ 4.62 (2H, H-1) correlates with an oxygenated carbon at δ 64.1 (C-1) and couples to an olefinic proton at δ5.76 (H-2). HMBC cross-peaks of H-1 with C-2 (δ 122.8), C-3 (δ 137.3), and C-1″ (δ 157.3) confirm this linkage. A singlet methyl proton at δ 1.78 (H-10) is correlated with C-2 (δ 122.8), C-3 (δ 137.3), and C-4 (δ 75.4). The ^{13}C NMR spectrum additionally shows one oxygenated methine carbon at δ60.7 (C-6) and one oxygenated tertiary carbon at δ 57.8 (C-7). The HMBC correlations of the methylene proton at δ 1.91 (H-5) with C-4, C-6, and C-7 suggest that H-5, adjacent to the epoxide group. The cross-peaks between two methyl groups of 8-CH_3 and 9-CH_3 with C-6 and C-7, and the triplet signal at δ 2.70 (H-6) characteristic of an epoxide proton, support the presence of a dimethyl-epoxide moiety attached at C-5. The remaining resonances corresponded to a saturated C16 fatty acid residue, which was palmitic acid. An ester carbonyl carbon at δ 172.8 (C-1′) and an HMBC correlation of H-4 (δ 5.37) with C-1′ confirmed the palmitoyloxy substitution at C-4. When the proton and carbon NMR data were compared with the published literature on servarine palmitate [17], they perfectly matched, and therefore, we have identified compound 1as servarine palmitate.

Compound 2 was also obtained as an amorphous white solid. Its purity (99.83%) was confirmed by HPLC analysis. The HR-ESI-MS data indicated a molecular formula of $C_{25}H_{31}NO_4$ (m/z 432.2156 $[M+Na]^+$; calcd. 432.2145). The IR spectrum showed absorption bands corresponding to an amide carbonyl (1637 cm^{-1}) and a broad hydroxyl group (3416 cm^{-1}). The ^{1}H and ^{13}C NMR data closely resembled those of compound 1, except for the absence of the fatty-acid chain at C-4, which showed the chemical shift at δ 75.2 (C-4) and δ 4.31 (H-4). When its chemical shifts were compared with its previously published proton and NMR data of acidissiminol epoxide [18], they matched exactly, and accordingly, we have identified compound 2 as acidissiminol epoxide.

Antiproliferative activity of A. monophylla crude extracts, fractions, and isolated compounds

We initially screened the inhibitory effects of *A. monophylla* extracts and fractions on the proliferation of human cancer cell lines and normal cells using the MTT colorimetric assay. A selectivity index (SI) greater than 3 was considered indicative of high selectivity. As shown in Table 1, cancer cells were exposed to various concentrations (1- 1,000 µg/mL) of three extracts-n-hexane, acetone, and methanol-for 72 hours. Among these, the acetone extract exhibited the strongest antiproliferative effects and the highest selectivity across all tested cell lines. The IC_{50} and SI values were as follow: HelaS3 (IC_{50} = 50.18 µg/mL, SI = 9.88), MCF-7 (IC_{50} = 46.26 µg/mL, SI = 10.71), HepG2 (IC_{50} = 58.87 µg/mL, SI = 8.42), and HCT116 (IC_{50} = 174.98 µg/mL, SI = 2.83). Additionally, it exhibited lower cytotoxicity toward Vero cells (IC_{50} = 495.65 µg/mL) compared with the n-hexane and methanol extracts (Table 1).

Due to its promising antiproliferative activity, the acetone extract was further fractionated into four fractions via silica gel column chromatography. Fraction 3, which showed notable antiproliferative activity against all tested cancer cell lines, particularly MCF-7, HepG2, and HCT116 cells, was selected for further chemical investigation. Two benzoyltyramine alkaloids, servarine palmitate (1) and acidissiminol epoxide (2), were isolated from the active acetone fraction of the peels of *A. monophylla* (Figure 1). Both compounds were again tested for their antiproliferative properties, and they both exhibited inhibitory effects against all tested cancer cell lines, with compound 2 demonstrating the strongest antiproliferative activity against MCF-7 cells (IC_{50} = 2.52 µg/mL) and showing the highest selectivity index (SI = 14.71). Based on these results, compound 2 was selected for further investigation of its anticancer mechanism of action.

Compound 2 induces apoptotic morphological alterations in MCF-7 cells

To determine whether the inhibitory effect of acidissiminol epoxide (compound 2) on the growth of MCF-7 cells is associated with apoptosis, we evaluated their apoptotic characteristics via several approaches, including morphological observations, DNA fragmentation via Hoechst 33342 staining, and cell cycle analysis using FACScan flow cytometry. First, we assessed the effects of compound 2 at concentrations of 10, 30, 100, and 300 µg/mL on the morphology of MCF-7 cells after 24 hours of exposure. Morphological changes were examined under phase-contrast and fluorescence microscopy following staining with the Hoechst 33342 kit. Compound 2 induced morphological alterations in MCF-7 cells, as shown in Figure 2. These changes were observed after 24 hours of exposure. A concentration-dependent effect was evident, with increasing doses of compound 2 (10–300 µg/mL) leading to prominent morphological changes. Compared with the control cells, the cells treated with 100 µg/mL and 300 µg/mL lost their typical shape, became rounded, and exhibited reduced adherence. Similarly, fluorescence microscopy via Hoechst 33342 staining revealed that compound 2 can induce apoptosis in breast cancer cells. The results of the present study revealed that, compared with untreated cells (Figure 3A), which displayed healthy morphology with no signs of apoptosis, increasing concentrations of compound 2 led to a corresponding increase in apoptosis.

This was characterized by cellular shrinkage, membrane blebbing, chromatin condensation, and the formation of apoptotic bodies (Figure 3B-E). Furthermore, treatment with the test compound at a relatively high concentration resulted in significant growth inhibition of cancer cells, whereas a relatively low concentration of the test compound led to a reduction in the number of cancer cells. Compound 2 is a potent molecule that induces chromatin condensation and nuclear fragmentation.

Flow cytometry analysis of the effects of compound 2 on cell cycle distribution/progression

Several studies have shown that apoptosis can be induced by cell cycle arrest; therefore, Inhibition of the cell cycle is recognized as a potential target for cancer therapy [20]. In the next step of this study, we evaluated whether treatment with compound 2 could induce apoptosis through cell cycle arrest. To explore the underlying mechanism of the effect of compound 2 on cell cycle progression, flow cytometric analysis was performed using PI staining (Figure 4A–B). The results revealed a significant increase in the G0/G1 phase population at concentrations of 10 and 30 µg/mL, indicating G0/G1 phase arrest. This was accompanied by a marked decrease in the S phase population, suggesting the inhibition of DNA synthesis and cell cycle progression. A moderate decrease in the G2/M phase was also observed at several concentrations. These findings suggest that compound 2 induces cell cycle arrest predominantly at the G0/G1 phase in a concentration-dependent manner, which may contribute to its antiproliferative effects on breast cancer cells.

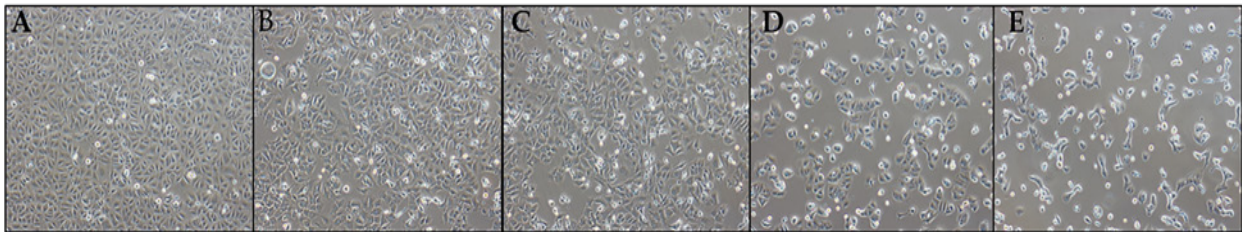

Figure 2. Morphological Characterization of MCF-7 Cell Lines Treated with (A) 0, (B) 10, (C) 30, (D) 100, and (E) 300 µg/mL of Compound 2 for 24 h.

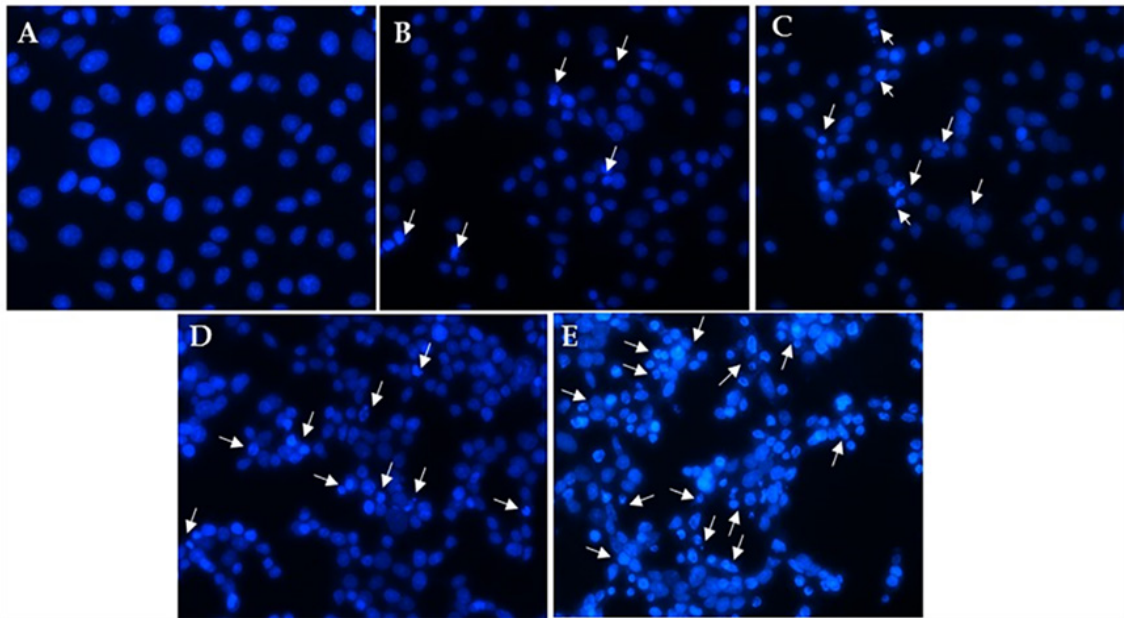

Figure 3. Compound 2 Induces Apoptosis in MCF-7 Cells. The cells were treated with (A) 0,(B) 10, (C) 30, (D) 100, and (E) 300 µg/mL of compound 2 for 24 h. The white arrows represent cells that underwent apoptosis. The images were captured via a fluorescence microscope (200x magnification).

Induction of apoptosis by compound 2 in MCF-7 cells

To quantify apoptotic cells after the treatment of MCF-7 cells with compound 2, a biparametric analysis was performed using an Annexin V and PI fluorescein staining kit, which stains phosphatidylserine residue and DNA, respectively, and then analyzed via flow cytometry. MCF-7 cells were treated with 10, 30, 100, and 300 µg/mL compound 2 for 24 h, followed by staining with Annexin V and propidium iodide using flow cytometry (Figure 5A). The untreated cells exhibited live cells (82.12±5.61%), necrosis (0.32±0.02%), late apoptosis (10.14±3.85%), and early apoptosis (7.38±2.54%). Conversely, the cells treated with compound 2 presented different cell populations at different stages, as shown in Figure 5B. Our study revealed that a greater population of 300 µg/mL treated cells underwent early apoptosis (18.03±3.03%), late apoptosis

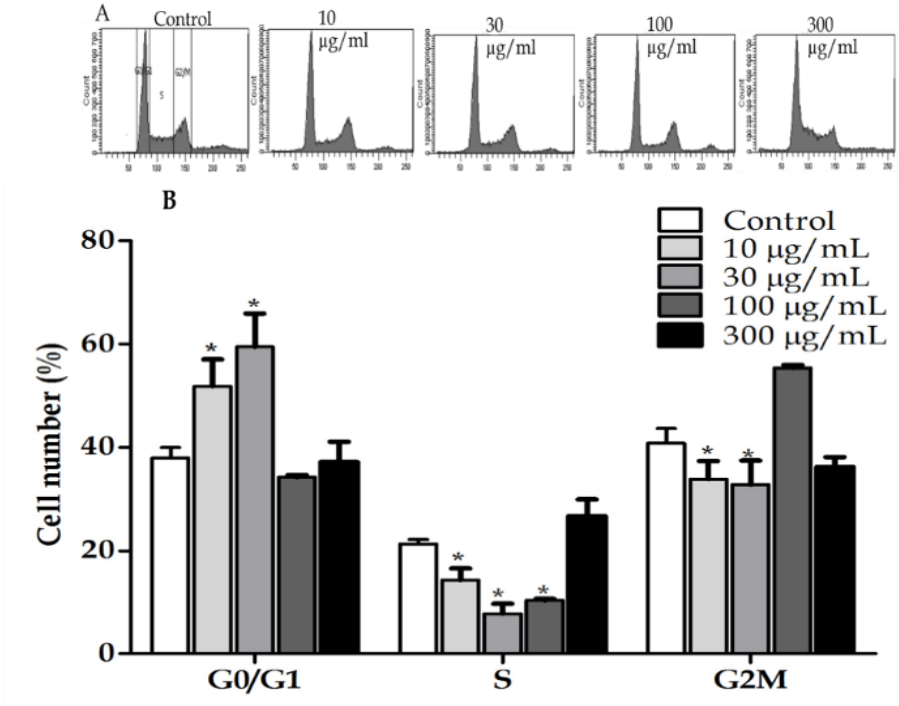

Figure 4. Effect of 2 Treatments on Cell Cycle Progression in MCF-7 Cells. After the MCF-7 cells were treated with 2 for 24 hours, they were stained with PI. (A) Representative flow cytometric histogram of cell cycle progression in MCF-7 cells after a particular treatment. (B) Bar graph displaying the percentage of the total population of cells. The values presented are the means ± SDs of three independent experiments.

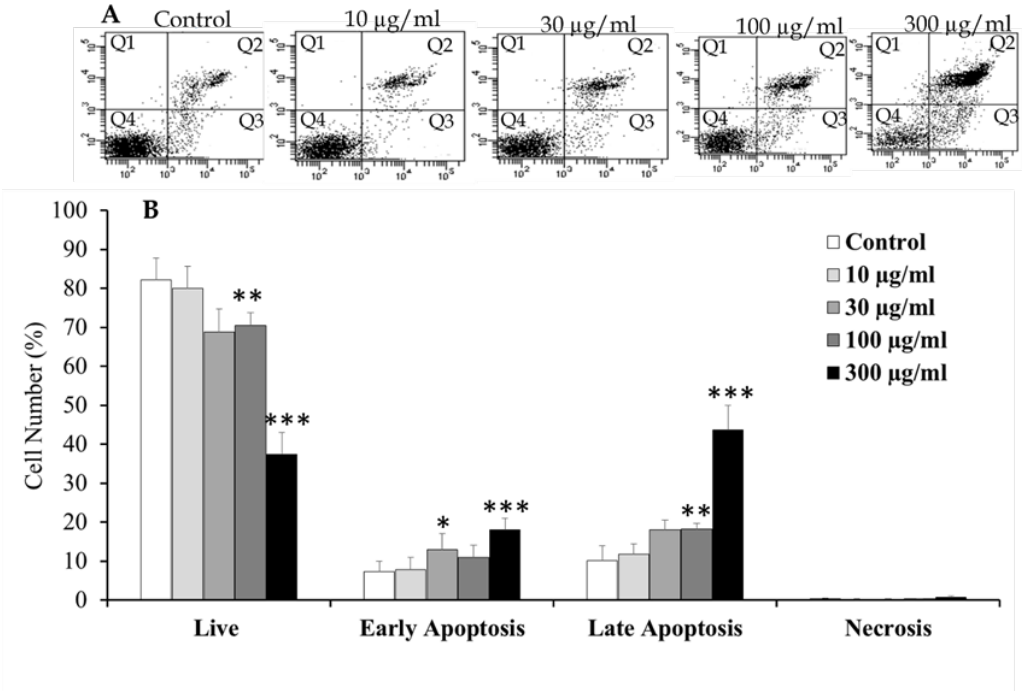

Figure 5. Effect of 2 on the Induction of Apoptosis in MCF-7 Cells. MCF-7 cells were treated with 2 for 24 h. (A) Annexin V-PI double-staining histogram showing apoptosis: Q1 necrosis; Q2 late apoptosis; Q3 early apoptosis; and Q4 viable cells. (B) Quantitative data analyses, with asterisks denoting levels of significance: * $p < 0.05$, ** $p < 0.01$, *** $p < 0.001$, vs. the untreated control.

(43.66±6.37%), and necrosis (0.32±0.05%), whereas 100 µg/mL significantly increased the percentage of apoptotic cells in late apoptosis (18.22±1.53%). Thus, compound 2 induced the externalization of phosphatidylserine and the loss of membrane integrity, leading to a dose-dependent increase in late apoptotic cells after treatment at the indicated concentrations. Taken together, these findings clearly confirm that compound 2 inhibited the proliferation of MCF-7 cells primarily by inducing G_0/G_1 phase arrest, which subsequently triggered apoptosis

Discussion

Although *A. monophylla* has been reported to possess significant pharmacological activities, including antibacterial, analgesic, anticancer, antipyretic, antidiabetic, and antihypertensive effects, to our knowledge, no detailed bioactivity studies have been conducted to date. In the present study, we report for the first time that peel extracts of *A. monophylla* can suppress breast cancer cell proliferation and induce apoptosis, as demonstrated through cell cycle and apoptosis analyses. Indeed, the acetone extract significantly inhibited the viability of MCF-7 cells in vitro compared with that of untreated cells. Bioactivity-guided chromatographic fractionation of the active acetone extract led to the isolation of two main isolated compounds and their characterization as epoxide moieties containing benzoyltyramine alkaloids, namely, servarine palmitate (1) and acidissiminol epoxide (2) (as shown in Figure 1). Interestingly, a search of the relevant literature revealed that tyramine alkaloid 2 was obtained for the first time from this plant. The cytotoxicity of compound 1 against HelaS3, MCF-7, HepG2, A549, HT116, and Vero cells was assessed via the MTT colorimetric assay (Table 1). Compound 1 was cytotoxic to all the tested cell lines and significantly inhibited various cancer cells but exhibited no cytotoxicity to normal cells. Additionally, the selectivity index (SI) of compound 1 was greater than three in HelaS3 cells (8.94), MCF-7 cells (9.20), and HepG2 cells (9.99). Surprisingly, compound 2, which contains a free hydroxyl group instead of a palmitoyloxy substituent at C-4, exhibited stronger cytotoxicity against all tested cell lines than compound 1. These findings revealed that the lack of a lipophilic long-chain palmitoyloxy group at C-4 may be critical for its cytotoxicity. However, the promising anticancer activity of both compounds 1 and 2 may be related to the presence of an epoxide ring in their structures. This feature is also found in some effective anticancer drugs from natural sources, such as carfilzomib, oprozomib, ixabepilone, and maytansine [21]. Interestingly, compound 2 also resulted in a high SI in HelaS3, MCF-7, HepG2, and HCT116 cells. Based on these results, Compound 2 was chosen for further investigation of its mechanism of action in terms of its anticancer activity.

Apoptosis plays a critical role in preserving cellular homeostasis by removing damaged or unnecessary cells. Numerous chemopreventive compounds have been shown to induce apoptosis as a means of eliminating cancer cells [22, 23]. Emerging studies highlight a strong association between apoptosis and both the development and progression of tumors [24, 25]. Consequently, enhancing apoptotic pathways is considered a key strategy in cancer therapy. Triggers such as cell cycle arrest, DNA damage, or cellular stress, either within the cytoplasm

or at the membrane level, can initiate apoptosis. In this study, the tested compounds demonstrated significant antiproliferative activity, particularly against MCF-7 breast cancer cells.

We hypothesized that acidissiminol epoxide (2) exerts its cytotoxic effects on cancer cells primarily through the induction of apoptosis. Consistent with this, classic morphological characteristics of apoptosis, such as membrane blebbing, cell shrinkage, chromatin condensation, nuclear fragmentation, apoptotic body formation, and loss of cell adhesion, were observed following 24 hours of treatment with the compound [20]. Flow cytometric analysis of the cell cycle revealed significant arrest at the G0/G1 phase (Figure 4), suggesting interference with DNA synthesis, a key process in cell cycle progression [20]. Importantly, the mechanistic studies did not include a standard chemotherapeutic agent as a positive control. As this investigation was designed as a preliminary screening of the antiproliferative and apoptosis-inducing potential of *A. monophylla* peel extract, the focus was placed on evaluating its intrinsic bioactivity.

Future studies should incorporate standard anticancer drugs to enable direct comparisons of efficacy and elucidation of mechanistic pathways. Additionally, Annexin V/PI staining combined with flow cytometry effectively differentiated apoptotic and necrotic cells from viable cells. Treatment with compound 2 led to a dose-dependent increase in both early and late apoptotic populations in MCF-7 cells. These findings support the conclusion that compound 2 induces apoptosis in breast cancer cells and that its antiproliferative activity is closely associated with this mechanism. Previous studies have also indicated that alkaloids can promote apoptosis through various cellular pathways [26, 27].

Our data further support the hypothesis that compound 2 inhibits the proliferation of MCF-7 cells by inducing cell cycle arrest and activating apoptotic cell death rather than necrosis. However, further detailed investigations are necessary to confirm these observations and fully elucidate the underlying mechanisms involved.

In conclusion, these observations indicate for the first time that the bioactivity-guided isolation of the peels of *A. monophylla* led to the isolation and identification of two known specific cytotoxic benzoyl tyramine alkaloids, namely, servarine palmitate (1) and acidissiminol epoxide (2). The present study demonstrated for the first time the antiproliferative effect of 2, which induced programmed cell death via the induction of DNA fragmentation, alteration of the cell cycle, and activation of apoptotic cells. However, such specificity needs to be proven by additional analyses, and the mechanism of targeting the apoptotic pathway remains unknown. However, further studies are needed to elucidate the active principle and validate these findings in various in vivo settings to develop it as a potential therapeutic agent for treating breast cancer.

Author Contribution Statement

All the authors contributed to the study idea and design, experimental work, paper writing, editing, and revision.

Acknowledgements

General

We are indebted to the Department of Chemistry, Faculty of Science, Silpakorn University, and the Department of Chemistry, Faculty of Science, Ramkhamhaeng University for recording NMR spectra and mass spectra, respectively. This research project was supported by Phetchaburi Rajabhat University (Fundamental Fund: the fiscal year 2023 by the National Science Research and Innovation Fund (NSRF), No. 179121).

Ethical Declaration

This study does not involve experiments on animals or human subjects.

Conflict of Interest

The study authors affirm that no conflicts of interest could influence the findings.

References

1. Giaquinto AN, Sung H, Miller KD, Kramer JL, Newman LA, Minihan A, et al. Breast cancer statistics, 2022. CA Cancer J Clin. 2022;72(6):524-41. https://doi.org/10.3322/caac.21754.
2. Zou H, Li Y, Liu X, Wu Z, Li J, Ma Z. Roles of plant-derived bioactive compounds and related micrornas in cancer therapy. Phytother Res. 2021;35(3):1176-86. https://doi.org/10.1002/ptr.6883.
3. Iqbal J, Abbasi BA, Mahmood T, Kanwal S, Ali B, Shah SA, et al. Plant-derived anticancer agents: A green anticancer approach. Asian Pac J Trop Biomed. 2017;7(12):1129-50. https://doi.org/10.1016/j.apjtb.2017.10.016.
4. Rayan A, Raiyn J, Falah M. Nature is the best source of anticancer drugs: Indexing natural products for their anticancer bioactivity. PLoS One. 2017;12(11):e0187925. https://doi.org/10.1371/journal.pone.0187925.
5. Govindachari TR, Viswanathan N, Pa BR, Ramachandran VN, Subramaniam PS. Alkaloids of *Atalantia monophylla* correa. Tetrahedron. 1970; 26(12): 2905-10. Https://doi.org/10.1016/s0040-4020(01)92869-8.
6. Bunyapraphatsara N., traditional herb. Thailand: Prachachon printinginc; 1999.
7. Panda H. Handbook on medicinal herbs with uses. Delhi: Asia pacific business INC; 2004.
8. Basa sc., atalaphyllinine, a new acridone base from *Atalantia monophylla*. Phytochemistry. 1975; 14(3): 835-6. Https://doi.Org/10.1016/j.Chemosphere.2008.12.034.
9. Baskar K, Kingsley S, Vendan SE, Paulraj MG, Duraipandiyan V, Ignacimuthu S. Antifeedant, larvicidal and pupicidal activities of *Atalantia monophylla* (l) correa against helicoverpa armigera hubner (lepidoptera: Noctuidae). Chemosphere. 2009;75(3):355-9. https://doi.org/10.1016/j.chemosphere.2008.12.034.
10. Patil vr, thakare v, joshi, vs. Immunomodulatory activity of *Atalantia monophylla DC*. Roots. Pharmacogn J. 2015; 7(1): 37-43. Http://dx.Doi.Org/10.5530/pj.2015.7.4. .
11. Das ak, swamy s. Antioxidant activity and determination of bioactive compound by GC-MS in fruit methanol extracts comparative analysis of three atalantia species from south india. J appl pharm sci. 2016; 6(2): 130-4. Https://doi.

Org/10.7324/japs.2016.60220.
12. Pailee P, Prawat H, Ploypradith P, Mahidol C, Ruchirawat S, Prachyawarakorn V. Atalantiaphyllines a-g, prenylated acridones from *Atalantia monophylla* DC. And their aromatase inhibition and cytotoxic activities. Phytochemistry. 2020;180:112525. https://doi.org/10.1016/j.phytochem.2020.112525.
13. Kumar TS, Krupadanam GL, Kumar KA. 5-hydroxydictamnine, a new alkaloid from *Atalantia monophylla*. Nat Prod Res. 2010;24(16):1514-7. https://doi.org/10.1080/14786419.2010.482052.
14. Posri P, Suthiwong J, Takomthong P, Wongsa C, Chuenban C, Boonyarat C, et al. A new flavonoid from the leaves of *Atalantia monophylla* (l.) dc. Nat Prod Res. 2019;33(8):1115-21. https://doi.org/10.1080/14786419.2018.1457667.
15. Sribuhom T, Boueroy P, Hahnvajanawong C, Phatchana R, Yenjai C. Benzoyltyramine alkaloids atalantums a-g from the peels of *Atalantia monophylla* and their cytotoxicity against cholangiocarcinoma cell lines. J Nat Prod. 2017;80(2):403-8. https://doi.org/10.1021/acs.jnatprod.6b00908.
16. Sombatsri A, Thummanant Y, Sribuhom T, Wongphakham P, Senawong T, Yenjai C. Atalantums h-k from the peels of *Atalantia monophylla* and their cytotoxicity. Nat Prod Res. 2020;34(15):2124-30. https://doi.org/10.1080/14786419.2019.1576042.
17. Dreyer dl, gigod jf, basa sc, mahanty p, das dp. Chemotaxonomy of the rutaceae-xii: The occurrence of severine in atalantia monophyla and hesperethusa crenulate. A revised structure for severine. Tetrahedron. 1980; 36(6): 827-9. Https://doi.Org/10.1016/s0040-4020(01)93701-9.
18. Ghosh P, Ghosh MK, Thakur S, Akihisa T, Tamura T, Kimura Y. Dihydroxy acidissiminol and acidissiminol epoxide, two tyramine derivatives from *Limonia acidissima.* Phytochemistry. 1994 Nov 14;37(3):757-60.
19. Chothiphirat A, Nittayaboon K, Kanokwiroon K, Srisawat T, Navakanitworakul R. Anticancer potential of fruit extracts from vatica diospyroides symington type ss and their effect on program cell death of cervical cancer cell lines. ScientificWorldJournal. 2019;2019:5491904. https://doi.org/10.1155/2019/5491904.
20. Kerr jer, winterford cm, harmon bv. Apoptosis, its significance in cancer and cancer therapy. Cancer. 1994; 73(8): 2013-26. Https://doi.Org/10.1002/1097-0142(19940415)73:8%3c2013::Aid-cncr2820730802%3e3.0.Co;2-j.
21. Gomes AR, Varela CL, Tavares-da-Silva EJ, Roleira FMF. Epoxide containing molecules: A good or a bad drug design approach. Eur J Med Chem. 2020;201:112327. https://doi.org/10.1016/j.ejmech.2020.112327.
22. Arumugam a, abdull raf. Apoptosis as a mechanism of the cancer chemopreventive activity of glucosinolates: A review. Asian pac j cancer prev. 2018; 19(6): 1439-48. Https://doi.Org/10.22034/apjcp.2018.19.6.1439.
23. Tanaka t. Role of apoptosis in the chemoprevention of cancer. J Exp Clin Med. 2013;5(3):89–91. Https://doi.org/10.1016/j.Jecm.2013.04.001.
24. Cooper GM, Hausman RE. The development and causes of cancer. The cell: a molecular approach. Darby S, Hill D, Auvinen A, Barros-Dios JM, Baysson H, Bochicchio F, Deo H, Falk R (2005) Radon homes risk lung cancer Collab Anal Individ data from. 2000;13:223-8
25. Kuang L, Wang L, Wang Q, Zhao Q, Du B, Li D, et al. Cudratricusxanthone g inhibits human colorectal carcinoma cell invasion by mmp-2 down-regulation through suppressing activator protein-1 activity. Biochem Pharmacol. 2011;81(10):1192-200. https://doi.org/10.1016/j.bcp.2011.02.017.
26. Mallick DJ, Korotkov A, Li H, Wu J, Eastman A. Nuphar alkaloids induce very rapid apoptosis through a novel caspase-dependent but bax/bak-independent pathway. Cell Biol Toxicol. 2019;35(5):435-43. https://doi.org/10.1007/s10565-019-09469-5.
27. Chen D, Ma Y, Guo Z, Liu L, Yang Y, Wang Y, et al. Two natural alkaloids synergistically induce apoptosis in breast cancer cells by inhibiting stat3 activation. Molecules. 2020;25(1). https://doi.org/10.3390/molecules25010216.